Inorganic Chemistry
Cite This: Inorg. Chem. 2018, 57, 899−902
Communication
pubs.acs.org/IC

Nanocoating of Hydrophobic Mesoporous Silica around MIL-101Cr for Enhanced Catalytic Activity and Stability

Jie Ying,[†] Annika Herbst,[‡] Yu-Xuan Xiao,[†] Hao Wei,[†] Ge Tian,[†] Zhaofei Li,[∥] Xiao-Yu Yang,*[,†] Bao-Lian Su,*[,†,§] and Christoph Janiak*[,‡]

[†]State Key Laboratory Advanced Technology for Materials Synthesis and Processing, Wuhan University of Technology, 122 Luoshi Road, Wuhan 430070, China

[‡]Institut für Anorganische Chemie und Strukturchemie, Heinrich-Heine-Universität Düsseldorf, 40204 Düsseldorf, Germany

[§]Laboratory of Inorganic Materials Chemistry (CMI), University of Namur, 61 rue de Bruxelles, B-5000 Namur, Belgium

[∥]Petrochemical Research Institute of Petrochina, Beijing 102206, China

Supporting Information

ABSTRACT: The metal−organic framework (MOF) MIL-101Cr was readily encapsulated by a very thin shell (around 30 nm) of hydrophobic mesoporous silica, which replicates the irregular shape of the MOF nanocrystals. Such a silica shell facilitates the diffusion of hydrophobic reactants with enhancement of the catalytic activity of the MOF and significantly improved catalytic stability of the MOF in the oxidation of indene.

Metal−organic frameworks (MOFs) have attracted widespread research interest, including as catalysts,[1−4] because of their ultrahigh surface area, tailorable porosity, and tunable composition.[5,6] However, many critical issues, such as the surface property and structure stability, must be addressed for the promise of their practical application.[7−9] Hierarchical nanoencapsulation has been considered to be an efficient approach to improving the stability of nanoparticles.[10−17] For example, a mesoporous silica ($mSiO_2$) shell can significantly enhance the mechanical properties of encapsulated nanosized MOFs.[12,18,19] However, it is still a great challenge to synthesis a hydrophobic mesoshell around nanocrystals because $mSiO_2$ usually exhibits strong hydrophilic properties. In spite of the improved stability of MOFs@silica,[20−22] there are only rare reports on their catalysis application.[23] Some attempts to render the surface of $mSiO_2$ hydrophobic, such as organic modification and surface roughening, have been successfully developed.[24−27] However, it is still not easy to change the hydrophilic surface property of mesostructured silica for the nanoencapsulation of MOFs because of the relatively harsh and/or complex procedure such as long-time and high-temperature reflux during the organic modification or secondary coating during the formation of a rough nanostructure.[24,27]

Herein, we present a simple method for the direct coating of MOF nanoparticles (MIL-101Cr) with a very thin hydrophobic $mSiO_2$ shell and investigation of the effect of the $mSiO_2$ shell on the MOFs in a catalytic application. MIL-101Cr[28] is a water-stable prototypical MOF[29,30] with interesting catalytic properties.[4] The silica shells can largely improve the stability of nanosized MOFs, and the larger mesopore size can allow chemical reactants or adsorbates to easily penetrate through this shell and reach the core without deteriorating the intrinsic properties of MOFs. Very interestingly, the very thin silica layer replicates the rough surface of an irregular MOF nanoparticle, resulting in a hydrophobic surface of $mSiO_2$. This unique feature enhances the catalytic activity and stability of MIL-101Cr during oxidation of indene. The core−shell-structured MIL-101Cr@$mSiO_2$ nanoparticles (designated as MIL-101Cr@$mSiO_2$) were prepared in three steps (Figure 1): (i) deposition of a thin

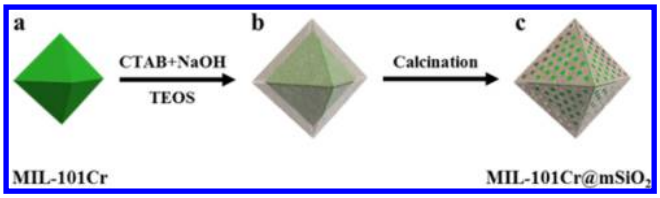

Figure 1. Schematic representation of the synthesis of MIL-101Cr@$mSiO_2$ sample.

intermediate micelle around the MIL-101Cr particles for (ii) the introduction and generation of the silica layer and (iii) removal of the surfactants by calcination to produce the MIL-101Cr@$mSiO_2$ particles with a $mSiO_2$ nanocoating (see the Supporting Information for details). The novelty in our work is the rational design of a hydrophobic $mSiO_2$ shell on an MOF with significantly improved catalytic stability and enhanced catalytic activity, whereas traditional $mSiO_2$-coated catalysts usually exhibit a close or lower activity in comparison to the bare catalysts because of the potential isolation and/or covering of active sites by the shell.

Transmission electron microscopy (TEM) and high-angle annular dark-field scanning TEM (HAADF-STEM) images of MIL-101Cr@$mSiO_2$ with energy-dispersive X-ray spectroscopy (EDX) element mapping show a core−shell structure, where each MIL-101Cr nanoparticle is encapsulated by a silica layer (Figure 2). The element Cr is distributed within the Si element shell. The thickness of the silica layer surrounding the MIL-101Cr core is around 30 nm. These results indicate that the composites with a core−shell structure are successfully

Received: August 4, 2017
Published: January 11, 2018

DOI: 10.1021/acs.inorgchem.7b01992
Inorg. Chem. 2018, 57, 899−902

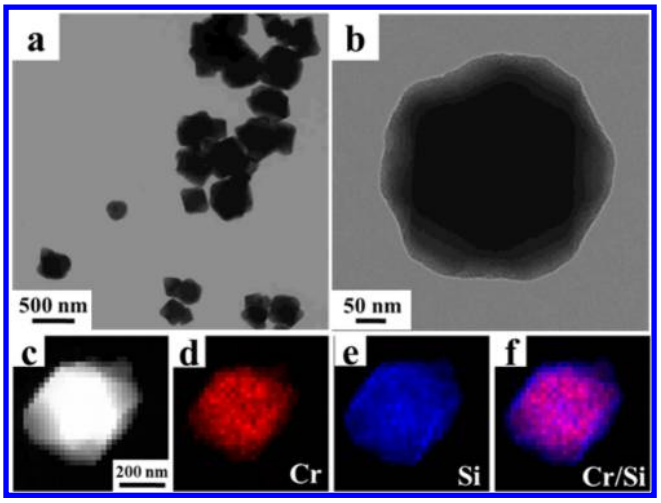

Figure 2. (a and b) Representative TEM images of MIL-101Cr@$mSiO_2$ samples at low and high magnification, respectively. (c) High-magnification HAADF-STEM image of a MIL-101Cr@$mSiO_2$ nanoparticle. Corresponding EDX elemental mapping results: (d) Cr (red); (e) Si (blue); (f) Cr and Si overlaid color mapping.

synthesized via the surfactant-directed coating route. Scanning electron microscopy (SEM) images of MIL-101Cr and MIL-101Cr@$mSiO_2$ also show similar irregular-to-octahedral morphology (Figure S1), indicating that the silica coating is very thin and replicates the MOF morphology.

From powder X-ray diffraction (XRD) patterns of MIL-101Cr and MIL-101Cr@$mSiO_2$ before and after calcination, the as-synthesized MIL-101Cr@$mSiO_2$ sample (Figure S2c) shows diffraction peaks similar to those of the MIL-101Cr sample (Figure S2b) and the simulated MIL-101Cr patterns (Figure S2a), suggesting retention of the framework structures during the silica coating process. The diffraction peaks of the MIL-101Cr@$mSiO_2$ sample (Figure S2d) display no change after careful calcination, demonstrating no significant destruction of the crystal structure of MIL-101Cr through the calcination process for removal of the surfactants. We cannot completely rule out that MIL-101Cr turns partly amorphous or is partly transformed into an amorphous decomposition product. However, work from others indicates that MIL-101Cr was stable up to 300 °C.[31−33] Here the calcination temperature for MIL-101Cr@$mSiO_2$ is only 250 °C, so we believe that MIL-101Cr can be stable and will retain its crystal structure during our calcination process. At the same time at 250 °C in vacuum overnight, the template surfactant cetyltrimethylammonium bromide (CTAB) will be decomposed and removed from the channels of silica. This is the common condition to remove the soft template CTAB or cetyltrimethylammonium chloride in the $mSiO_2$ channels.[12]

The N_2 sorption isotherms and pore-size distributions of the MIL-101Cr and MIL-101Cr@$mSiO_2$ samples are illustrated in Figure S3 and Table S1. Pure MIL-101Cr shows the characteristic type I(b) isotherm with the characteristic step between $0.1 < p/p_0 < 0.2$ because of the presence of two kinds of microporous windows/mesoporous cages (Figure S3a).[28] After coating with $mSiO_2$ shells, the MIL-101Cr@$mSiO_2$ sample shows a mixed isotherm (Figure S3b), in which $mSiO_2$ and microporous MIL-101Cr are both effective for the isotherm curvature, and the isotherm should be assigned as a nonclassical type IV. The pore-size distribution of MIL-101Cr@$mSiO_2$ reflects the same distinct pores as those in MIL-101Cr but with one more pore at around 2.8 nm (Figure S3c), which can be attributed to the $mSiO_2$ shell (Figure S4). The specific Brunauer−Emmett−Teller surface area of 1156 $m^2\ g^{-1}$ for MIL-101Cr@$mSiO_2$ is slightly less than the mass-weighted expected value of 1408 $m^2\ g^{-1}$ (see Figure S3 and the accompanying text in the Supporting Information).

The catalytic property of MIL-101Cr@$mSiO_2$ was evaluated toward the oxidation of indene with H_2O_2 in acetonitrile (see Figure S5 for the reaction scheme), a valuable reaction of the oxidation of alkenes to carboxylic acids in organic synthesis.[34] Figure 3a shows the conversion of indene against time after

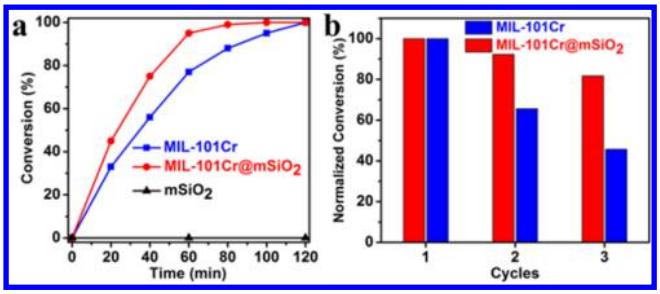

Figure 3. (a) Time-domain conversion of indene by MIL-101Cr, MIL-101Cr@$mSiO_2$, and $mSiO_2$. (b) Comparison of the conversion for MIL-101Cr and MIL-101Cr@$mSiO_2$ over three reaction runs. The reaction time is 80 min.

addition of the catalysts. As can be seen, both MIL-101Cr and MIL-101Cr@$mSiO_2$ samples are effective catalysts for the oxidation reaction. The activity of MIL-101Cr@$mSiO_2$ is obviously higher than that of the MIL-101Cr sample, and the turnover frequency (TOF) value (Table S2) of the MIL-101Cr@$mSiO_2$ sample (95.2 mmol $g^{-1}\ h^{-1}$) is 1.24 times greater than that of the MIL-101Cr sample (76.8 mmol $g^{-1}\ h^{-1}$). For example, after 1 h, the conversion of indene with the MIL-101Cr@$mSiO_2$ sample is 95%, while the conversion with the MIL-101Cr sample is only 77%. Pure $mSiO_2$ and also H_2O_2 alone cannot oxidize indene under the same reaction conditions. Thus, the enhanced catalytic activity of MIL-101Cr@$mSiO_2$ can be ascribed to the structure advantage of the $mSiO_2$ shell, which allows for faster diffusion of the reactants and products (for the effect of the silica shell thickness on conversion, see Figure S6 and the accompanying text).[35,36]

We note that the improvement of the catalytic conversion is significant beyond doubt. Thereby we also point to the catalytic experiments, which were performed in triplicate to exclude larger deviations and to ensure data reliability (Table S3). We used the average values in the conversion diagrams in Figure 3. In this proof-of-principle study, we note that it is not necessarily expected to improve the catalyst conversion of MOFs constrained in porous structures. In our case, the catalytic activity of MIL-101Cr for the oxidation of indene could be obviously enhanced by rationally covering them with a hydrophobic $mSiO_2$ shell. Catalysts encapsulated within a silica shell usually exhibit a close or lower activity in comparison to the bare catalysts because of the potential isolation and/or covering of active sites by the shell together with diffusion limitations. Moreover, the catalytic stability of MIL-101-Cr has been improved significantly. Altogether, this is a surprising result. Here, the $mSiO_2$ shell could obviously enhance the catalytic activity of MIL-101Cr for the oxidation of indene although the diffusion rate of molecules through the silica shell should be slowed, and fewer active sites in the silica-enclosed MIL-101Cr may be available.

The increase in catalytic activity for MIL-101Cr@$mSiO_2$ is counterintuitive. So the reason for the enhanced activity by the

DOI: 10.1021/acs.inorgchem.7b01992
Inorg. Chem. 2018, 57, 899−902

silica shell needed to be more deeply investigated. Notably, the catalytic substrate (indene, is a hydrophobic reactant), is insoluble in water and dissolved in organic acetonitrile solution while MIL-101Cr is of intermediate hydrophilicity−hydrophobicity as based on water vapor uptake versus relative pressure in adsorption measurements.[29,30] In comparison water vapor sorption indicates that $mSiO_2$ is more hydrophobic.[37] The hydrophilic−hydrophobic property of $mSiO_2$ can be readily tuned by surface roughness engineering, such that $mSiO_2$ nanospheres with a smooth surface show hydrophilicity. Rough $mSiO_2$ nanospheres with the same hydrophilic composition show unusual hydrophobicity.[27] So it is believed that the roughness of $mSiO_2$ (see below) could result in hydrophobic $mSiO_2$ and we supposed that the $mSiO_2$ shell would facilitate the exchange between hydrophobic reactants and the embedded MOF catalysts by providing a possibly hydrophobic intermedium around MIL-101Cr. To support this hypothesis, the hydrophilic−hydrophobic property of the nanoparticles was characterized by the dispersion behavior of MIL-101Cr@$mSiO_2$ and MIL-101Cr in a two phase decane-water system. As seen from Figure 4a, MIL-101Cr@$mSiO_2$ collected at the bottom of the

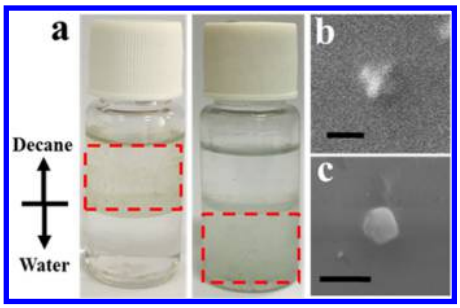

Figure 4. (a) Dispersion behavior of MIL-101Cr@$mSiO_2$ (left) and MIL-101Cr (right). The high-magnification SEM images of (b) MIL-101Cr@$mSiO_2$ and (c) MIL-101Cr on a PDMS layer for measuring individual contact angles by the GTT method (see the Supporting Information for further details). Scale bars are 300 nm.

hydrophobic decane layer after adding nanoparticles with mild shaking while MIL-101Cr collected at the bottom of the water layer. This indicates that MIL-101Cr@$mSiO_2$ is hydrophobic while the MIL-101Cr is hydrophilic. Furthermore, indene adsorption experiments show that MIL-101Cr@$mSiO_2$ adsorbs indene more readily than MIL-101Cr (Figure S7). Moreover, a gel-trapping technique (GTT)[38−40] was used to provide a more direct comparison of the hydrophilic−hydrophobic properties between MIL-101Cr@$mSiO_2$ and MIL-101Cr because the traditional contact-angle measurement for film surfaces does not easily apply for nanoparticles as their sizes are much smaller than that of a liquid droplet. A schematic presentation of the GTT preparation protocol for the contact-angle measurement of MIL-101Cr@$mSiO_2$ and MIL-101Cr is shown in Figure S8.

The hydrophilic−hydrophobic properties of nanoparticles can be judged by their position on the poly(dimethylsiloxane) (PDMS) layer as the nanoparticles were picked up from the decane/water interfaces. Individual MIL-101Cr@$mSiO_2$ is mostly embedded in the PDMS film (Figure 4b), indicating the hydrophobicity of the $mSiO_2$ shell. On the contrary, individual MIL-101Cr is mostly visible on the PDMS surface (Figure 4c), showing the higher hydrophilicity of MIL-101Cr. Possibly, the hydrophobicity of $mSiO_2$ is due to a rough nanostructure[27] caused by the very thin silica copy of the irregular shape of MIL-101Cr (see Figure S9 and the accompanying text). To rule out the presence of hydrophobic hydrocarbon residues on the surface of MIL-101Cr@$mSiO_2$, see Figure S10 and S11 and the accompanying text.

To extend MIL-101Cr@$mSiO_2$ to other reactions with both hydrophobic and hydrophilic substrates, the oxidation of 1-dodecene in acetonitrile (Figure S12) and the dehydration of glucose in water (Figure S13) were conducted. As expected, MIL-101Cr@$mSiO_2$ exhibits a higher activity than MIL-101Cr toward the hydrophobic dodecene substrate (Figure S14) but a lower activity than MIL-101Cr toward the hydrophilic glucose substrate (Figure S15).

As shown in Figure 3b, the reusability of MIL-101Cr@$mSiO_2$ in indene oxidation is much better than that of MIL-101Cr. After three runs, 82% of the initial conversion is retained for MIL-101Cr@$mSiO_2$, but only 46% of the initial conversion is still present for MIL-101Cr, indicating that the $mSiO_2$ shell significantly enhances the catalytic stability of the embedded MIL-101Cr sample in the oxidation of indene. The XRD patterns of MIL-101Cr@$mSiO_2$ before and after three reaction cycles show no obvious differences (Figure S16), demonstrating the high structural stability of MIL-101Cr@$mSiO_2$.

In conclusion, the MOF MIL-101Cr incorporated in a hydrophobic $mSiO_2$ shell has been readily synthesized. The MIL-101Cr@$mSiO_2$ sample exhibits enhanced catalytic activity and improved reusability as a catalyst in the oxidation of indene. This study shows a unique effect of a hydrophobic $mSiO_2$ shell on MOFs for the catalytic transformation of hydrophobic organic substrates.

■ ASSOCIATED CONTENT

Supporting Information

The Supporting Information is available free of charge on the ACS Publications website at DOI: 10.1021/acs.inorgchem.7b01992.

Experimental details, SEM, XRD, N_2 adsorption/desorption, GTT protocol, and tables (PDF)

■ AUTHOR INFORMATION

Corresponding Authors

*E-mail: xyyang@whut.edu.cn.
*E-mail: bao-lian.su@fundp.ac.be.
*E-mail: janiak@uni-duesseldorf.de.

ORCID

Christoph Janiak: 0000-0002-6288-9605

Notes

The authors declare no competing financial interest.

■ ACKNOWLEDGMENTS

This work was supported by the National Key R&D Program of China (2017YFC1103800), NSFC (U1663225, U1662134, 51472190, 51611530672, 51503166, and 51611530672), ISTCP (2015DFE52870), PCSIRT (IRT_15R52), HPNSF (2016CFA033 and 2017CFB487), BMBF Project OptiMat 03SF0492C, and the DAAD through PPP Project 57053987 (China 2j ab 14).

■ REFERENCES

(1) Corma, A.; García, H.; Llabrés i Xamena, F. Engineering Metal Organic Frameworks for Heterogeneous Catalysis. *Chem. Rev.* **2010**, *110*, 4606−4655.
(2) Chughtai, A. H.; Ahmad, N.; Younus, H. A.; Laypkov, A.; Verpoort, F. Metal-Organic Frameworks: Versatile Heterogeneous Catalysts for

DOI: 10.1021/acs.inorgchem.7b01992
Inorg. Chem. 2018, 57, 899−902

Efficient Catalytic Organic Transformations. *Chem. Soc. Rev.* **2015**, *44*, 6804−6849.
(3) Liu, J.; Chen, L.; Cui, H.; Zhang, J.; Zhang, L.; Su, C.-Y. Applications of Metal−Organic Frameworks in Heterogeneous Supramolecular Catalysis. *Chem. Soc. Rev.* **2014**, *43*, 6011−6061.
(4) Herbst, A.; Janiak, C. MOF Catalysts in Biomass Upgrading towards Value-Added Fine Chemicals. *CrystEngComm* **2017**, *19*, 4092−4117.
(5) Murray, L. J.; Dincă, M.; Long, J. R. Hydrogen Storage in Metal−Organic Frameworks. *Chem. Soc. Rev.* **2009**, *38*, 1294−1314.
(6) Yang, X.-Y.; Chen, L.-H.; Li, Y.; Rooke, J. C.; Sanchez, C.; Su, B.-L. Hierarchically Porous Materials: Synthesis Strategies and Structure Design. *Chem. Soc. Rev.* **2017**, *46*, 481−558.
(7) Kitagawa, S.; Kitaura, R.; Noro, S. i. Functional Porous Coordination Polymers. *Angew. Chem., Int. Ed.* **2004**, *43*, 2334−2375.
(8) Rowsell, J. L.; Yaghi, O. M. Metal−Organic Frameworks: a New Class of Porous Materials. *Microporous Mesoporous Mater.* **2004**, *73*, 3−14.
(9) Janiak, C.; Vieth, J. K. MOFs, MILs and More: Concepts, Properties and Applications for Porous Coordination Networks (PCNs). *New J. Chem.* **2010**, *34*, 2366−2388.
(10) Lu, G.; Li, S.; Guo, Z.; Farha, O. K.; Hauser, B. G.; Qi, X.; Wang, Y.; Wang, X.; Han, S.; Liu, X.; et al. Imparting Functionality to a Metal−Organic Framework Material by Controlled Nanoparticle Encapsulation. *Nat. Chem.* **2012**, *4*, 310−316.
(11) Wang, P.; Zhao, J.; Li, X.; Yang, Y.; Yang, Q.; Li, C. Assembly of ZIF Nanostructures around Free Pt Nanoparticles: Efficient Size-Selective Catalysts for Hydrogenation of Alkenes under Mild Conditions. *Chem. Commun.* **2013**, *49*, 3330−3332.
(12) Li, Z.; Zeng, H. C. Armored MOFs: Enforcing Soft Microporous MOF Nanocrystals with Hard Mesoporous Silica. *J. Am. Chem. Soc.* **2014**, *136*, 5631−5639.
(13) Yang, X. Y.; Li, Y.; Van Tendeloo, G.; Xiao, F. S.; Su, B. L. One-Pot Synthesis of Catalytically Stable and Active Nanoreactors: Encapsulation of Size-Controlled Nanoparticles within a Hierarchically Macroporous Core@Ordered Mesoporous Shell System. *Adv. Mater.* **2009**, *21*, 1368−1372.
(14) Ying, J.; Yang, X.-Y.; Hu, Z.-Y.; Mu, S.-C.; Janiak, C.; Geng, W.; Pan, M.; Ke, X.; Van Tendeloo, G.; Su, B.-L. One Particle@One Cell: Highly Monodispersed PtPd Bimetallic Nanoparticles for Enhanced Oxygen Reduction Reaction. *Nano Energy* **2014**, *8*, 214−222.
(15) Ying, J.; Hu, Z.-Y.; Yang, X.-Y.; Wei, H.; Xiao, Y.-X.; Janiak, C.; Mu, S.-C.; Tian, G.; Pan, M.; Van Tendeloo, G.; Su, B.-L. High Viscosity to Highly Dispersed PtPd Bimetallic Nanocrystals for Enhanced Catalytic Activity and Stability. *Chem. Commun.* **2016**, *52*, 8219−8222.
(16) Ying, J.; Jiang, G.; Paul Cano, Z.; Han, L.; Yang, X.-Y.; Chen, Z. Nitrogen-Doped Hollow Porous Carbon Polyhedrons Embedded with Highly Dispersed Pt Nanoparticles as a Highly Efficient and Stable Hydrogen Evolution Electrocatalyst. *Nano Energy* **2017**, *40*, 88−94.
(17) Huang, G.; Yang, Q.; Xu, Q.; Yu, S. H.; Jiang, H. L. Polydimethylsiloxane Coating for a Palladium/MOF Composite: Highly Improved Catalytic Performance by Surface Hydrophobization. *Angew. Chem., Int. Ed.* **2016**, *55*, 7379−7383.
(18) Zhu, Q.-L.; Xu, Q. Metal−Organic Framework Composites. *Chem. Soc. Rev.* **2014**, *43*, 5468−5512.
(19) Zhan, G.; Zeng, H. C. Integrated Nanocatalysts with Mesoporous Silica/Silicate and Microporous MOF. *Coord. Chem. Rev.* **2016**, *320-321*, 181−192.
(20) Rieter, W. J.; Taylor, K. M.; Lin, W. Surface Modification and Functionalization of Nanoscale Metal-Organic Frameworks for Controlled Release and Luminescence Sensing. *J. Am. Chem. Soc.* **2007**, *129*, 9852−9853.
(21) Taylor-Pashow, K. M.; Della Rocca, J.; Xie, Z.; Tran, S.; Lin, W. Postsynthetic Modifications of Iron-Carboxylate Nanoscale Metal−Organic Frameworks for Imaging and Drug Delivery. *J. Am. Chem. Soc.* **2009**, *131*, 14261−14263.
(22) Taylor, K. M.; Rieter, W. J.; Lin, W. Manganese-Based Nanoscale Mmetal−Organic Frameworks for Magnetic Resonance Imaging. *J. Am. Chem. Soc.* **2008**, *130*, 14358−14359.
(23) Sachse, A.; Ameloot, R.; Coq, B.; Fajula, F.; Coasne, B.; De Vos, D.; Galarneau, A. In Situ Synthesis of Cu-BTC (HKUST-1) in Macro-/Mesoporous Silica Monoliths for Continuous Flow Catalysis. *Chem. Commun.* **2012**, *48*, 4749−4751.
(24) Lu, J.; Liong, M.; Zink, J. I.; Tamanoi, F. Mesoporous Silica Nanoparticles as a Delivery System for Hydrophobic Anticancer Drugs. *Small* **2007**, *3*, 1341−1346.
(25) Yamashita, H.; Kawasaki, S.; Yuan, S.; Maekawa, K.; Anpo, M.; Matsumura, M. Efficient Adsorption and PhotoCatalytic Degradation of Organic Pollutants Diluted in Water Using the Fluoride-Modified Hydrophobic Titanium Oxide Photocatalysts: Ti-Containing Beta Zeolite and TiO_2 Loaded on HMS Mesoporous Silica. *Catal. Today* **2007**, *126*, 375−381.
(26) Vallet-Regí, M.; Colilla, M.; González, B. Medical Applications of Organic−Inorganic Hybrid Materials within the Field of Silica-Based Bioceramics. *Chem. Soc. Rev.* **2011**, *40*, 596−607.
(27) Ahmad Nor, Y.; Niu, Y.; Karmakar, S.; Zhou, L.; Xu, C.; Zhang, J.; Zhang, H.; Yu, M.; Mahony, D.; Mitter, N.; Cooper, M. A.; Yu, C. Shaping Nanoparticles with Hydrophilic Compositions and Hydrophobic Properties as Nanocarriers for Antibiotic Delivery. *ACS Cent. Sci.* **2015**, *1*, 328−334.
(28) Férey, G.; Mellot-Draznieks, C.; Serre, C.; Millange, F.; Dutour, J.; Surblé, S.; Margiolaki, I. A Chromium Terephthalate-Based Solid with Unusually Large Pore Volumes and Surface Area. *Science* **2005**, *309*, 2040−2042.
(29) Ehrenmann, J.; Henninger, S. K.; Janiak, C. Water Adsorption Characteristics of MIL-101 for Heat-Transformation Applications of MOFs. *Eur. J. Inorg. Chem.* **2011**, *2011*, 471−474.
(30) Khutia, A.; Rammelberg, H. U.; Schmidt, T.; Henninger, S.; Janiak, C. Water Sorption Cycle Measurements on Functionalized MIL-101Cr for Heat Transformation Application. *Chem. Mater.* **2013**, *25*, 790−798.
(31) Bhattacharjee, S.; Chen, C.; Ahn, W.-S. Chromium Terephthalate Metal−Organic Famework MIL-101: Synthesis, Functionalization, and Applications for Adsorption and Catalysis. *RSC Adv.* **2014**, *4*, 52500−52525.
(32) Pascanu, V.; Yao, Q.; Bermejo Gómez, A.; Gustafsson, M.; Yun, Y.; Wan, W.; Samain, L.; Zou, X.; Martín-Matute, B. Sustainable Catalysis: Rational Pd Loading on MIL-101Cr-NH_2 for More Efficient and Recyclable Suzuki-Miyaura Reactions. *Chem. - Eur. J.* **2013**, *19*, 17483−17493.
(33) Cao, N.; Su, J.; Luo, W.; Cheng, G. Ni−Pt Nanoparticles Supported on MIL-101 as Highly Efficient Catalysts for Hydrogen Generation fromAqueous Alkaline Solution of Hydrazine for Chemical Hydrogen Storage. *Int. J. Hydrogen Energy* **2014**, *39*, 9726−9734.
(34) Saedi, Z.; Tangestaninejad, S.; Moghadam, M.; Mirkhani, V.; Mohammadpoor-Baltork, I. MIL-101 Metal−Organic Framework: a Highly Efficient Heterogeneous Catalyst for Oxidative Cleavage of Alkenes with H_2O_2. *Catal. Commun.* **2012**, *17*, 18−22.
(35) Park, J. C.; Song, H. Metal@Silica Yolk-Shell Nanostructures as Versatile Bifunctional Nanocatalysts. *Nano Res.* **2011**, *4*, 33−49.
(36) Sun, J.; Bao, X. Textural Manipulation of Mesoporous Materials for Hosting of Metallic Nanocatalysts. *Chem. - Eur. J.* **2008**, *14*, 7478−7488.
(37) Wang, D.; Zhang, J.; Yang, Q.; Li, N.; Sumathy, K. Study of Adsorption Characteristics in Silica Gel-Water Adsorption Refrigeration. *Appl. Energy* **2014**, *113*, 734−741.
(38) Paunov, V. N.; Cayre, O. J. Supraparticles and "Janus" Particles Fabricated by Replication of Particle Monolayers at Liquid Surfaces Using a Gel Trapping Technique. *Adv. Mater.* **2004**, *16*, 788−791.
(39) Paunov, V. N. Novel Method for Determining the Three-Phase Contact Angle of Colloid Particles Adsorbed at Air-Water and Oil-Water Interfaces. *Langmuir* **2003**, *19*, 7970−7976.
(40) Cayre, O. J.; Paunov, V. N. Contact Angles of Colloid Silica and Gold Particles at Air-Water and Oil-Water Interfaces Determined with the Gel Trapping Technique. *Langmuir* **2004**, *20*, 9594−9599.

DOI: 10.1021/acs.inorgchem.7b01992
Inorg. Chem. 2018, 57, 899−902